Green Chemistry

ARTICLE

Epimerization of glucose over ionic liquid/phosphomolybdate hybrids: structure-activity relationship

Received 00th January 20xx,
Accepted 00th January 20xx

DOI: 10.1039/x0xx00000x

www.rsc.org/

Cristina Megías-Sayago,*[a] Eleuterio Álvarez,[b] Svetlana Ivanova[a] and José Antonio Odriozola[a] †

The influence of the crystal structure and chemical nature of some ionic liquid/phosphomolybdate hybrids on their catalytic activity in the epimerization of glucose is studied. A clear evidence for structure-activity relationship is found. The inorganic part of the hybrid assures the active sites for the reaction; meanwhile the organic cation nature organizes the structure and controls the diffusion of the reactants. This study can be used as a first approach to predict the symmetry, long range order and active sites availability of the presented class of imidazolium based polyoxometalate hybrids.

Introduction

Biomass feedstock valorization includes a great number of chemical transformations to useful products, among which carbohydrate/sugars epimerization supposes an important step. The epimerization of aldoses, such as glucose, arabinose or xylose, at C2 position involves the sugar conversion to its chiral counterpart. This glucose transformation to its epimer, mannose (Scheme 1), received much less attention than its isomerization into fructose, a fact explaining that only few chemocatalytic systems have been discovered for selective epimerization.[1]

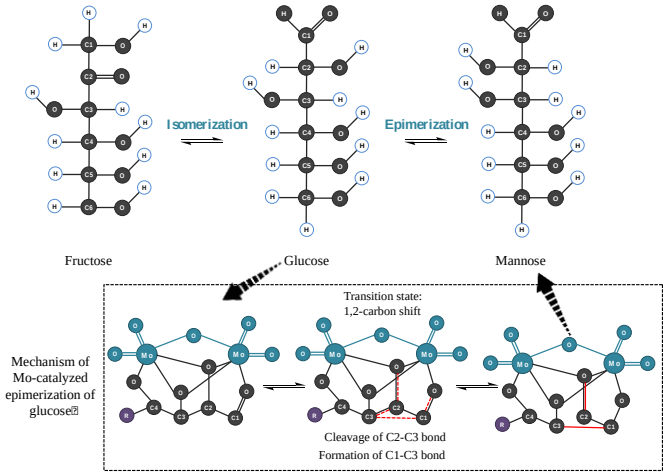

Scheme 1. Glucose epimerization *vs.* isomerization. Reaction mechanism of Mo-catalyzed epimerization of glucose.

[a] Departamento de Química Inorgánica e Instituto de Ciencia de Materiales de Sevilla, Centro mixto CSIC-Universidad de Sevilla, Avda. Americo Vespucio 49, 41092 Sevilla, Spain. *Email: cristina.megias@icmse.csic.es
[b] Instituto de Investigaciones Químicas, Centro mixto CSIC-Universidad de Sevilla, Avda. Americo Vespucio 49, 41092 Sevilla, Spain

†Electronic Supplementary Information (ESI) available: See DOI: 10.1039/x0xx00000x

Both, isomerization and epimerization occurs in presence of basic or Lewis acid catalysts,[2–4] although the formation of the corresponding ketose predominates in most systems. The formation of fructose via isomerization requires small reorganization of the intermediate, whereas the formation of mannose takes place through rotation around the C_2-C_3 bond (see Scheme 1). This difference may be the reason why the formation of mannose is generally slower in comparison to the glucose to fructose reaction.[5] Both reactions, however, are limited by thermodynamics, being 50:50 the reported Glucose/Fructose isomerization equilibrium[6] and 70:30 Glucose/Mannose equilibrium ratio.[7]

The epimerization is broadly used for different processes, including production of rare sugars and pharmaceuticals.[8–10] Currently, epimer production is assured by epimerases, highly selective in the epimerization of carbohydrates at different carbon positions. However, the number of drawbacks derived from the use of enzyme-catalyzed processes at industrial level, such as, sensitivity to temperature and pH, operating window restriction, and difficult post reaction separation promotes the search for solid inorganic catalysts.[11] Basic catalysts such as $Ca(OH)_2$ and NaOH have been reported for the epimerization of glucose to mannose.[1] However, it has been demonstrated that, in basic conditions, a series of 50 different secondary products can be formed, diminishing selectivity to the desired epimer.[12,13] In a similar way, the epimerization process may occur via complexation of the substrate with Ni/diamines complexes,[14,15] being the reaction limited by the thermodynamics of the intermediate complex formation, which implies the use of large quantities of catalyst.[16]

The most studied process for efficient aldoses epimerization is known as Bilik reaction.[17–20] In 1970s Bilik discovered that molybdate anions in acidic media can epimerize glucose to mannose at 90 ºC attaining thermodynamic equilibrium in 3h of reaction, without fructose formation.[4] The catalysts activity, however, was strongly influenced by the pH: the maximum yields were registered at pH 2.0-3.5,[21] being this pH necessary to maximize the concentration of dimeric Mo^{VI} species,[21] considered as the active ones. The rate of epimerization drastically decreases on increasing pH, which entails the use of stronger Brönsted acid sites,

provided by mineral acids addition. The epimerization follows a carbon-shift mechanism passing through coordination of the substrate onto Mo^{VI} dimer (Scheme 1), simultaneous cleavage of the C_2-C_3 carbon bond and the formation of new C_1-C_3 carbon bond, all steps confirmed by ^{13}C NMR.[19] Through this mechanism, a large amount of compounds can be selectively epimerized, when the alkylic chain presents at least four carbons and hydroxyl groups in C_2, C_3 and C_4 positions. The importance of the Bilik reaction was rapidly recognized and scaled up to pilot plant running in Bratislava. At this point, the challenge to make more efficient the overall process is to find an active and stable molybdate solid acid catalyst.

VanderVelde and coworkers[11] recently reported for the first time the use of phosphomolybdic acid and Ag/Sn based salts in the above mentioned reaction, resulting in near-equilibrium conversions with high selectivity within 60 min. The registered conversions are independent of the nature of cations (H^+, Ag^+, Sn^{4+}), suggesting that the cation does not participate in the process. Isotope-labelling ^{13}C NMR confirms that the reaction follows the above mentioned 1,2-carbon shift mechanism.[11] The use of Keggin polyoxometalates (POMs) for aldose epimerization is really attractive, since the needed tandem active species/Brönsted sites are present, thereby avoiding additional mineral acid utilization. Furthermore, POMs salts nature enable their heterogeneous use, highly desirable from economic and environmentally points of view.[22] Several strategies to prepare heterogeneous POM catalysts have been applied, mainly based on the loading of the structure onto porous supports.[23–26] However, recently, the organic-inorganic hybrid POM compounds emerge as a promising way to form heterogeneous POMs[27–29] with tunable properties derived from the high number of possible organic ligands and resulting structures after combining them with the metal oxide cluster. Generally, the POMs structure is considered as potential Brönsted site, whereas the introduction of an organic ligand increases the porosity of the structure and provides a convenient way to modify the polarity of the framework. For all these reasons the use of hybrid structures presents an advantage over the POM salts for the application in the epimerization reaction.

In this work we propose three different hybrid structures based on the same Keggin (phosphomolybdic) anion but different type of alkyl imidazolium ionic liquid (IL), concretely 1-ethyl-3-methylimidazolium methanesulfonate, 1-butyl-3-methylimidazolium methanesulfonate and 1-hexyl-3-methylimidazolium chloride. In all cases, the organic cations are constituted by 3-methyl substituted imidazolium ring, differing in their 1-alkyl substituent. Adopted nomenclature refers to the number of carbons in the latter, [C2mim], [C4mim] and [C6mim], respectively. PMoA is used to denote the proton compensated Keggin cluster (phosphomolybdic acid - $H_3PMo_{12}O_{40}$) and [C2mim]PMo, [C4mim]PMo, [C6mim]PMo denote the corresponding hybrid salt formed by the combination of each IL with PMoA. The resulting molecular formula is $[Cxmim]_3[PMo_{12}O_{40}]$ with all protons of the original acid substituted by organic cations. Their structures were studied by conventional and small angle XRD and the crystallographic parameters and assemblies of the three molybdenum-based hybrids determined by single crystal XRD. For one chosen hybrid $[C2mim]_3[PX_{12}O_{40}]$, the transition metal centers of the Keggin anions were varied, resulting in two additional structures $[C2mim]_3[PW_{12}O_{40}]$, and $[C2mim]_5[PMo_{10}V_2O_{40}]$, labelled [C2mim]PW and [C2mim]PMoV, respectively. The catalytic behavior of all compounds in glucose epimerization reaction is studied and related to the nature of the hybrid. A relationship between the hybrid channel structure and activity is established and discussed. Reaction parameters such as time and temperature are evaluated. Recycling study is also considered.

Results and discussion

The formation of organic-inorganic hybrid POM is usually described as self-assembling process difficult to predict in structure and composition[22,30] due to the complex behavior of POM - organic counterion interaction during crystallization. A controlled design and synthesis of this kind of hybrids is still an important challenge due to the variety of structures that can be originated taking into account the diversity of conformations resulting from different organic fractions (different molecular weight, chemical composition and chain lengths).[31–35] The XRD diffractograms of all synthesized compounds are presented in Fig. 1. XRD pattern of PMoA corresponds to hydrated phosphomolybdic acid $H_3PMo_{12}O_{40}\cdot 13H_2O$ (JCPDS #01-075-1588) crystalizing in triclinic structure in agreement with literature.[36] The PMoA displayed a set of well-resolved diffractions of typical secondary organization of a Keggin type crystal.[37] The introduction of different organic fractions leads to similar diffractions within the 7- 40° range, suggesting intact Keggin structure in the hybrids. Nevertheless, a shift in the existing diffractions and also some new appeared, accounting for the presence of organic cation and some modifications of the structure. It should be noted that the longest alkylic chain hybrid [C6mim]PMo present a sharp diffraction at small angles, around 6°, normally indicative for long-range ordering. As reported,[38] some ionic liquids in solid state form an extended cooperative network of cations and anions, connected through hydrogen bonds. This 3D arrangements in the case of imidazolium ILs give rise to “free” volumes with high degree of directionality, known as ionic self-assemblies (ISA).[30] The changes of the XRD profiles appear to be related to the type of cation being the XRD profile of [C2mim]PMo more similar to the parent acid than [C4mim]PMo and [C6mim]PMo. Shorter the aliphatic chain, the smaller the modification of the parent acid diffractogram.

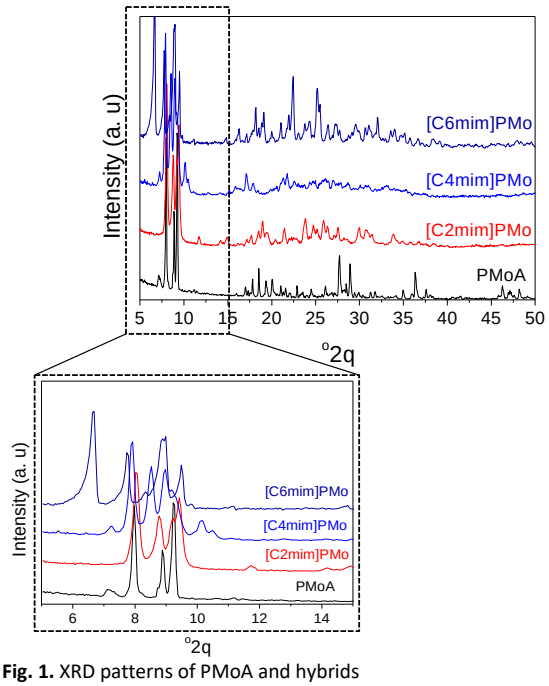

Fig. 1. XRD patterns of PMoA and hybrids

The presence of low-angle diffractions for [C6mim]PMo hybrid suggested formation of species with certain long-order arrangements. A small angle X ray diffraction experiment (Figure 2) reveals the existence of large interplanar spacing increasing from C2 to C6 hybrid. According to the Bragg law, the spacings move from 11Å to 11.2Å and 13.3Å (Cu K-alpha = 1.5418 Å) for C2, C4 and C6, respectively. Thereby the formation of long-range order organic-inorganic compounds is a function of the length of the substitute alkyl chain. One interesting question arises at this point: Is it possible to predict the interplanar spacing, knowing the number of the aliphatic carbons? In order to check that, two new Mo hybrids with C12 and C16 alkyl substitute chains are prepared. As shown in Fig. 2A small angle diffractions appear in both cases and the interplanar spacing move from 28.6Å to 36.8Å for C12 and C16, respectively. Therefore, it is clear that the structure organization is induced by the ionic liquid nature. Almost linear relationship was obtained between the number of the carbons in the alkyl chain and the *d*-spacing of the resulting hybrid (Fig. 2B). At low carbon number (2 to 4) the structure resembles the original Keggin structure, whereas at higher carbon number (> 6 carbons) the steric hindering/electrostatic repulsions become important, resulting in longer distances and long-range order appearance. The latter was confirmed by the single-crystal structural analysis. The three hybrids crystalized in three-dimensional structures containing $[Cxmim]_3PMo_{12}O_{40}$ frameworks without included water molecules. The ORTEP representations of the molecular salts are shown in Fig. 3A, Fig. 4A and Fig. 5A, respectively and Table S1 (Supporting Information) includes all obtained crystallographic data, such as crystal system, space group, unit cell parameters (axes and angles), unit volume and number of molecular unit in the unit cell.

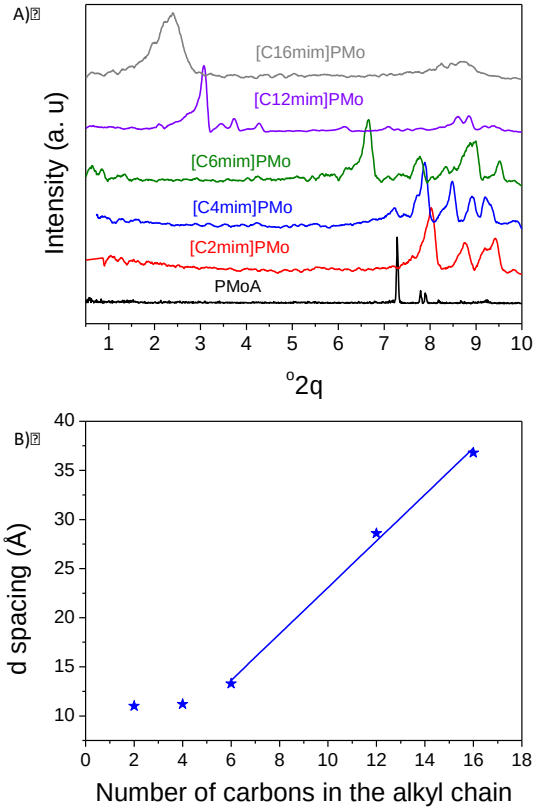

Fig. 2. A) Small angle X ray diffractograms of Mo based hybrids (including C12 and C16) and B) *d*-spacing/number of carbons correlation

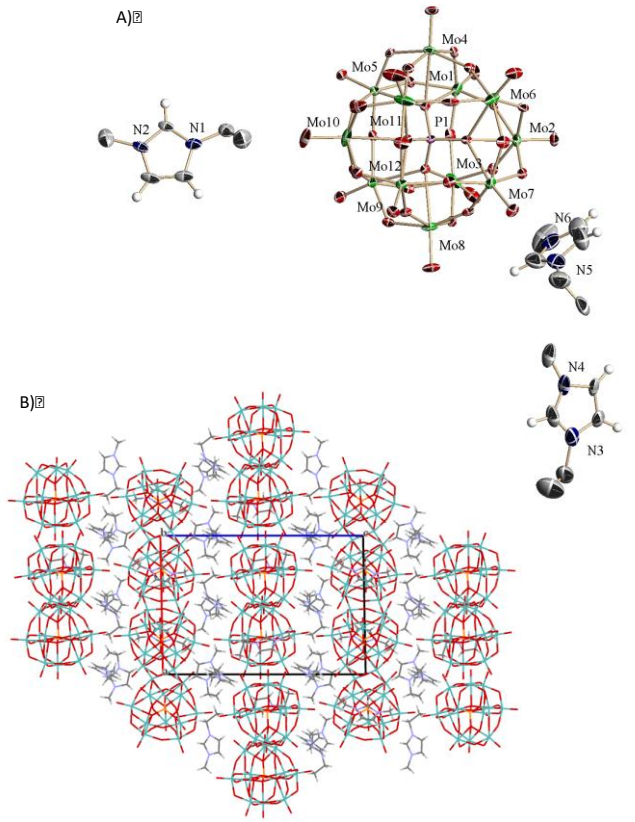

Fig. 3. A) ORTEP diagram drawing at 30% probability level. Hydrogen atoms were omitted for clarity. B) Packing diagram (view along the crystallographic *b*-axis) for [C2mim]PMo

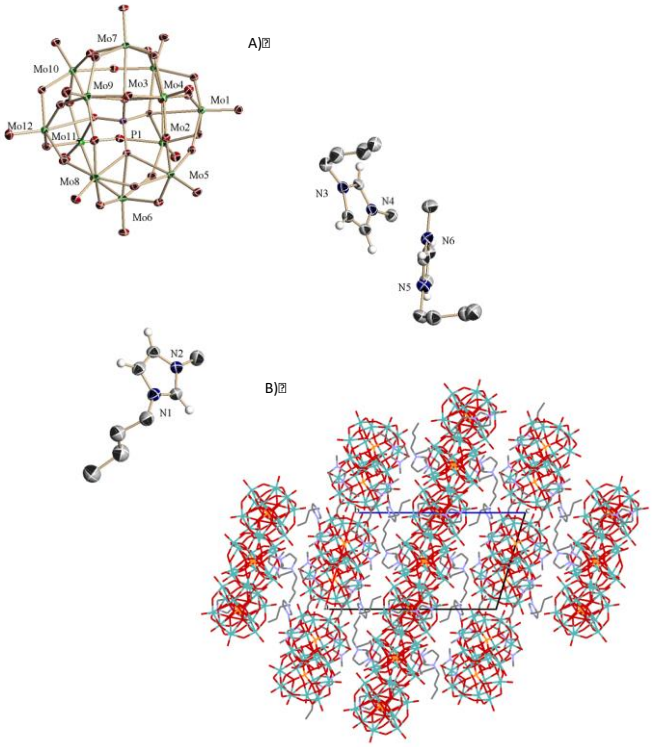

Fig. 4. A) ORTEP diagram drawing at 30% probability level. Hydrogen atoms were omitted for clarity. B) Packing diagram (view along the crystallographic *b*-axis) for [C4mim]PMo

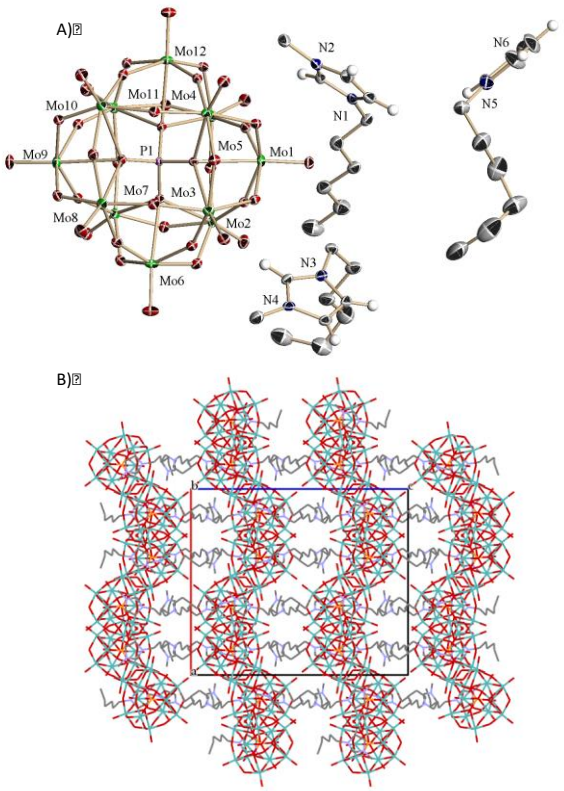

Fig. 5. A) ORTEP diagram drawing at 30% probability level. Hydrogen atoms were omitted for clarity. B) Packing diagram (view along the crystallographic *b*-axis) for [C6mim]PMo

Both [C2mim]PMo and [C4mim]PMo crystallize in P-1 space group, with 4 molecular units per unit cell. The expanded structure packings are shown in Fig. 3B and 4B respectively. Both hybrids show the same space group as the original acid (JCPDS #01-075-1588). On the contrary, [C6mim]PMo crystallizes in Pbca space group, with 4 molecular units per unit cell. The increase of the carbon numbers in the aliphatic chain of the cation increases the symmetry of the final compounds and induces the long range organization as shown by the SAXRD results (Figure 2). The structure directionality is different for C2mim, C4mim (Fig. 3B, Fig. 4B) and C6mim (Fig. 5B) hybrids, *e.g.* different channels exist formed upon cations – anions arrangement. [C2mim]PMo and [C4mim]PMo presents parallel channels along *a* direction, whereas the [C6mim]PMo structure is organized in a *zig-zag* way. It is clear that the cation introduction to the Keggin anion leads to the formation of different tridimensional structures with structural features directly related with the number of carbons present as imidazolium ring substitutes. Shorter aliphatic chain gives rise to more open structures: the channels formed between Keggin units are less occupied by the corresponding organic cations. The latter could be demonstrated through planar density calculations, where some considerations should be taken into account to simplify and compare the three structures: i) both cations and anions are considered as one atom and the plane refers to all atoms within 10Å thickness (Figure S1A); ii) {001} family is used iii) the plane area is the same in all cases and iv) the considered space is taken at same coordinates origin (as shown in Fig. S1B for [C2mim]PMo).

Planar densities of the three hybrids are calculated by using eq. 1. and resulted in 1.1, 3 and 4 atoms per nm^2 for [C2mim]PMo, [C4mim]PMo and [C6mim]PMo, respectively. It is therefore, evident, that shorter aliphatic chains give rise to less compact structures directly related to the cation occupation of the channels.

$$PD_{001} = \frac{number\ of\ atoms\ centered\ on\ (001)\ plane}{area\ of\ (001)\ plane} \qquad \text{Eq. 1.}$$

Catalytic activity studies

Aldose conversions for the three hybrids based on phosphomolybdic acid as a function of the reaction temperature are presented in Figure 6. An increase of glucose conversion with temperature is observed. When compared to literature data[11,39,40] (Table S2; entries 2, 3 and 4) the results observed for [C2mim]PMo correspond to the reported equilibrium conversions. Undeniably, glucose to mannose conversion strongly depends on organic cation nature, in a way that longer the substitute aliphatic chain, lower the glucose conversion, following the trend [C2mim]PMo > [C4mim]PMo > [C6mim]PMo. Considering that the anionic part of the hybrid is the same for the three samples the observed catalytic behavior suggests that either the IL cations are participating directly in the reaction or that the hybrid structural organization is responsible for the differences. If the cation participates actively in the reaction the H^+ substituted PMoA sample (bare acid) should show different behavior. However, the catalytic performance of PMoA leads to identical conversion data (Table 1; entry 1) as the corresponding [C2mim]PMo salt (Table 1; entry 2). The pure ionic liquid does not catalyze the glucose transformation neither (Table 1; entry 7) which leads to the conclusion that the IL cation is not involved in the reaction.

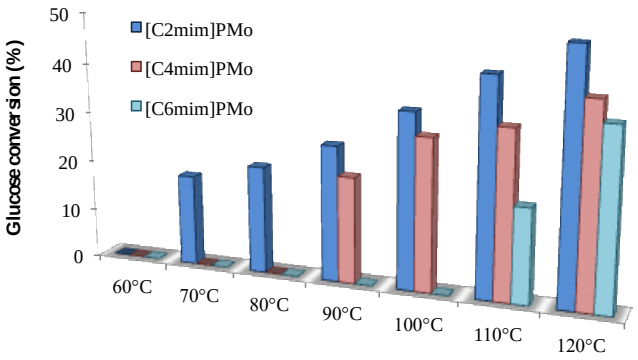

Fig. 6. Glucose conversion (%) as function of the reaction temperature for the PMoA based hybrids.

Table 1. Catalytic performance of different hybrids in the epimerization of glucose

Entry	Catalyst [a]	χ (%)	S [b] (%)	pH[c]
1	PMoA	48	100	1.87
2	[C2mim]PMo	49	100	2.72
3	[C4mim]PMo	40	100	-
4	[C6mim]PMo	35	100	-
5	[C2mim]PW	0	0	2.62
6	[C2mim]PMoV	55	73	3.80
7	$[C2mim](SO_3)CH_3$ [d]	0	0	-

[a]Reaction conditions: 5 mL of 0.2 M glucose solution, Glucose:hybrid 256:1 molar ratio (1:0.05 Glucose:Metal ratio), 120 ºC, 60 min and 600 rpm. [b] Selectivity reported as mannose+fructose selectivity. [c] pH not controlled during reaction, measured at t = 0. [d] The IL amount is equivalent to the corresponding hybrid loading in this conditions.

As for the hybrids' structure organization, it is convenient to discuss the activity in terms of crystallographic structure. Attending to the Mo hybrids expanded structures, the [C2mim]PMo presents the less compact structure of cations providing better aldose diffusion path to the active sites and less steric impediments for the formation of molybdenum-glucose complex. The lower planar density calculated for this hybrid could also account for hybrid' less hydrophobic nature, higher affinity to glucose molecules and maximal thermodynamic conversion at low temperatures. Therefore, the catalytic activities are directly correlated with the availability of Mo^{VI} active centers, as reported by VanderVelde for homologous POMs.[11] Based on the latter, the activity trend [C2mim]PMo > [C4mim]PMo > [C6mim]PMo is congruent with [C4mim]PMo and [C6mim]PMo long-range structures and cavities dimensions restriction (see Figures 3, 4 and 5).

[C2mim]PW and [C2mim]PMoV and their corresponding acids $H_3PW_{12}O_{40}$ (PWA) and $H_5PMo_{10}V_2O_{40}$ (PMoVA) were also studied and compared to molybdenum based acid and hybrid at 120 ºC (Table 1, entries 5 and 6). Despite the fact that 1,2-carbon shift has been reported only for Mo compounds, W and V based hybrids could become potential alternatives as they form also heteropolyanions with the same structure as molybdenum. This study is also motivated by the fact that molybdates, tungstates and vanadates are very effective for the glucose metabolism *in vivo*. The use of these metals results in lowering of the glucose blood levels and helps to control the diabetes.[41,42] The three metals show similar sensitivity to glucose and form similar Metal-glucose complexes[41] with similar characteristics and logically should catalyze one or more glucose transformation reactions.[43] Additionally the change of the metal center induces variation in acidity.

The observation made for [C2mim]PW and [C2mim]PMoV hybrids (Table 1, entries 5 and 6, respectively) clearly evidenced the influence of the anion' metal center. Whereas replacing Mo with W resulted in activity loss, the replacing of two Mo with V leads to conversion improvement. Nevertheless, the selectivity to mannose decreases in favor to glyceraldehyde (27 % selectivity). Glyceraldehyde is a product of fructose retro-aldolic condensation, reaction which takes place also on Lewis acid sites[44] under acidic conditions. The glyceraldehyde formation indirectly suggests formation of fructose.

At this point, it is very important to pay all our attention to the reaction selectivity. Under our HPLC operation conditions, mannose and fructose are eluted at the same retention time, which makes impossible the proper calculation of the selectivity. Although the molybdate-based compounds has been reported as 100% selective toward epimerization at low reaction times, catalytic test at 80 ºC over [C2mim]PMo was carried out again to contrast it. After the reaction the catalyst was separated and the products lyophilized and re-dissolved in deuterium oxide for ^{13}C {^1H} NMR characterization (Figure S2). The obtained chemical shifts are contrasted with reported values as summarized in Table S3.

Before the reaction, only glucose was detected, while after reaction, only new signals identified. In all cases, both α and β conformations are presents due to the existing equilibriums between axial and equatorial substituents in aqueous solution.[45] The new signals agree with the presence of α- and β-mannose. No evidence of fructose presence within the reacted mixture was observed (Table S3, entries 5 and 6). The absence of resonance at 100 ppm (Table S3, entries from 7 to 10) corresponding to fructose C2 and also signals in the 80-90 ppm range, due to C3 (α-conformation) and C5 (α- and β-conformation) confirms mannose as the only reaction product at this temperature, a 100 % of glucose epimer was achieved.

This result is consistent with the study of Hayes and coworkers[7] where 100 % of selectivity over molybdenum systems is observed at short reaction times. However, at longer reaction times secondary products can be formed. Glucose conversion over [C2mim]PMo as a function of reaction time at the same reaction conditions (80 ºC, 600 rpm), is presented in Figure 7. After 60 min of reaction, the conversion almost attains the equilibrium concentration and after 2 hours of reaction all registered conversions exceed the equilibrium value, entailing most probably the formation of secondary products. From the HPLC measurements could be deduced that the secondary product corresponds only to fructose, since no new products appear but the intensity of the mannose+fructose HPLC signal increases, in agreement with the reports of Hayes *et al.*[7] and Bilik.[46] Once the epimerization equilibrium reached, the unconverted glucose can undergo intramolecular hydride shift in the presence of the molybdate-glucose complex[46] resulting in reaction of glucose isomerization. As described previously, both, glucose epimerization and isomerization take place over Lewis acid and basic catalysts, although in most cases, the isomerization prevails. It seems that over the hybrid Mo systems like [C2mim]PMo hybrid, the epimerization prevails at short reaction times. Once the equilibrium attained, the hydride shift reaction takes place, giving rise to further fructose formation. Still, more studies are required and will be the object of future works.

One of the great challenges in this process when carried out homogeneously is catalyst separation and reutilization, an essential requisite to make any process economically viable. Despite that the organic cations seem to act as spectators during the epimerization, its role is as important as the anion action. Their presence converts the used materials in solids, insoluble in aqueous solvents, feature that makes possible their separation and reutilization. The viability of the [C2mim]PMo catalyst was evaluated by reusing it three times at 80 ºC during 60 min, without any treatment between the cycles (Fig. 8). In all cases, the water-to-glucose-to-catalyst ratio was kept constant to ensure the same reaction conditions. The recycled catalyst exhibits similar activity to that of the original sample, suggesting that hybrid's decomposition does not occur under those

specific reaction conditions (Figure S4). Slight improvement of activity was observed in the 2nd and 3d cycle, due probably to the partial reduction of Mo after the first cycle (confirmed by change of hybrids color form yellow to blue) and facilitating the first step of the reaction, i.e. the electron transfer. However, this statement and possible implication in reaction mechanism still need additional study.

Conclusions

The hybrids formed by inorganic anions and organic cations interactions are new structural materials with preserved Keggin inorganic structure. Long-range order organization appears for those compounds and becomes more evident on increasing the imidazolium ring substituents alkyl chain length. Crystallographic data reveals three-dimensional structures containing $[Cxmim]_3PMo_{12}O_{40}$ frameworks, in which channels and cavities are formed due to the alternate organization of cations and anions. The latter is related with the number of carbon atoms in the alkyl chain present in the imidazolium ring: the shorter chain hybrids organize in less compact structures.

The less compact hybrids are highly active and selective for the epimerization of glucose at low reaction times. The organic cations do not participate in the carbon shift mechanism; however, their presence influences the overall process indirectly by the organization of hybrid' structure and channel system. Smaller cations give rise to less compact structures for improved glucose diffusion and metal availability, whereas longer chain cations exert negative effect on the metal-glucose complex formation and glucose epimerization activity.

The presence of different Keggin anion metal centers also influences the activity and selectivity of the systems. The substitution of Mo with W leads to important activity loss whereas the substitution of two atoms of Mo by V causes the formation of other products like glyceraldehyde, indirect evidence for fructose formation at higher reaction times.

Finally, it has been demonstrated that the hybrid structures do not decompose under the proposed reaction conditions and can be easily extracted from the solution and efficiently recycled in a number of cycles.

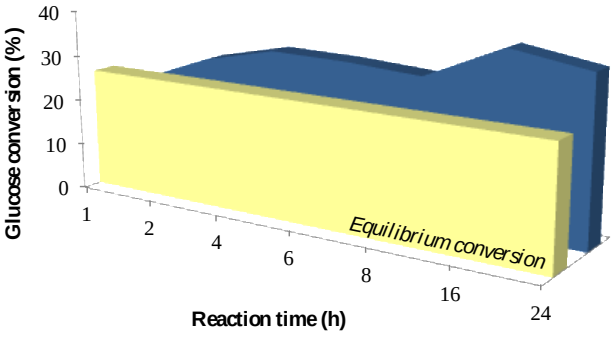

Fig. 7. Glucose conversion (%) as a function of the reaction time. Reaction conditions: 1 mmol of glucose, 0.4 mol% of [C2mim]PMo, 80 ºC and 600 rpm

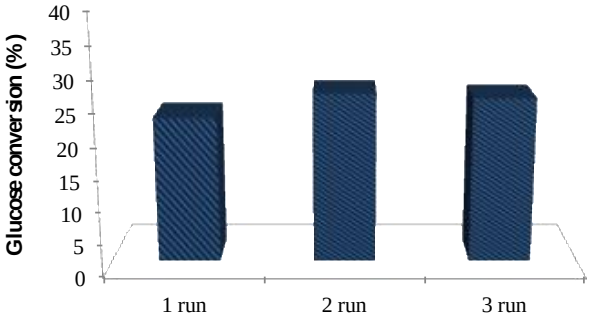

Fig. 8. Recycling experiments over [C2mim]PMo.

Experimental

Catalysts preparation

The proton compensated POM cluster *i.e.* phosphomolybdic acid - $H_3PMo_{12}O_{40}$ (PMoA), was synthesized as previously reported.[47] For the hybrid synthesis, three commercial alkyl imidazolium ionic liquids (ILs) were used, 1-ethyl-3-methylimidazolium methanesulfonate (Alfa Aesar), 1-butyl-3-methylimidazolium methanesulfonate (Sigma Aldrich) and 1-hexyl-3-methylimidazolium chloride (Alfa Aesar). PMoA was combined with each IL, resulting in three different hybrid structures as proposed in the literature.[48–50] The amount of PMoA and IL was adjusted to preserve the 3:1 IL:POM molar ratio. The method of preparation, detailed below for $[C2mim]_3[PMo_{12}O_{40}]$, is analogous for all solids: appropriate quantities of PMoA (0.9 g) and 1-ethyl-3-methylimidazolium methanesulfonate (0.34 g) were separately dissolved in distilled water. Under controlled mixing, a precipitate of the POM-IL hybrid appeared. The precipitate was separated by filtration and dried at room temperature. Following this procedure, the all other hybrid structures were obtained. All the hybrids were used as prepared without any additional treatment.

Single crystals of Mo based hybrids were obtained in order to determine the crystallographic parameters of the resulting structures. Completely dried hybrids were recrystallized from an equal volume (10 + 10 mL) mixture of acetone and acetonitrile. Solvents were carefully evaporated at room temperature for 7 days, and yellow monocrystals were formed and used for single crystal X-ray diffraction analysis.

Characterization

Conventional XRD experiments were carried out on an X'Pert Pro PANalytical diffractometer, using Cu K_α (40 mA, 45 kV) as source of radiation. The diffractograms were recorded over the 5 to 50° 2θ range with 0.05° step size and acquisition time of 300 s.

Small angle X-ray diffraction (SAXRD) experiments were performed in an X'Pert Pro Philips diffractometer equipped with Cu anode (K_α, 40 mA, 45 kV). The diffractograms were recorded over 0.5 - 10.0° 2θ range with 0.01° step size and acquisition time of 1.5 s.

Single crystal X-ray diffraction (SCXRD) analysis were performed on a Bruker-Nonius X8APEX-II CCD diffractometer using monochromated-graphite radiation ??(Mo K?) = 0.71073 Å by means of ω and ? scans with a width of 0.50 degree. The structures were resolved using direct methods with a SIR 2004[51] and refined against all F^2 data by full-matrix least-squares techniques (SHELXL-2016/6) minimizing $w[F_o^2-F_c^2]^2$.[52] The hydrogen atoms were included from calculated positions and refined riding on their respective carbon atoms with isotropic displacement parameters. Some geometric restraints (DFIX instruction), the ADP restraint SIMU and the rigid bond restraint DELU were used to make the geometric and ADP values of the disordered atoms more reasonable. CCDC 1590119 - 1590121 (for [C2mim]PMo, [C4mim]PMo and [C6mim]PMo, respectively) contain the supplementary crystallographic data for this paper. These data can be obtained free of charge from The Cambridge Crystallographic Data Centre via www.ccdc.cam.ac.uk/data_request/cif.

^{1}H and ^{13}C NMR were employed to determinate the species in the post reaction liquid mixture. For this purpose, the final reaction mixture was lyophilized in a Flexi-Dry P FTS System lyophilizer and re-dissolved in deuterium oxide. This experiment was performed in a Bruker Avance DRX-400.

Catalytic tests

All the reactions were conducted at atmospheric pressure in a glass batch reactor of 50 mL capacity provided with a small magnetic stirring bar and a young valve. The epimerization reaction was performed in 5 ml of total volume in which glucose (1 mmol, 0.1802 g) and hybrid catalyst in a Glucose:hybrid 256:1 molar ratio were mixed with 5 ml of H_2O. The mixture was heated in paraffin oil bath with carefully controlled temperature and stirring rate of approximately 600 rpm. After reaction, the mixture was cooled down in an ice bath and a sample taken, microfiltered and diluted in ultra-pure water for analysis. The product analysis was performed on Varian 360 Liquid Chromatograph provided with a Hi-Plex H column (300 × 7.7 mm), a refractive index detector and by using 0.01M H_2SO_4 as eluent.

Conflicts of interest

There are no conflicts to declare

Notes and references

1 I. Delidovich, R. Palkovits, *ChemSusChem*, 2016, **9**, 547.
2 R. Yanagihara, S. Osanai, S. Yoshikawa, *Chem. Lett.*, 1990, **19**, 2273.
3 S. Osanai, R. Yanagihara, K. Uematsu, A. Okumura, S. Yoshikawa, *J. Chem. Soc. Perkin Trans.,* 1993, **2**, 1937.
4 V. Bilik, *Chem. Zvesti.*, 1972, **26,** 183.
5 G. De Wit, A.P.G. Kieboom, H. van Bekkum, *Carbohydr. Res.,* 1979, **74,** 157.
6 Y.B. Tewari, *Appl. Biochem. Biotechnol.,* 1990, **23,** 187.
7 M.L. Hayes, N.J. Pennings, A.S. Serianni, R. Barker, *J. Am. Chem. Soc.,* 1982, **104,** 6764.
8 T. Granström, G. Takata, M. Tokuda, I. K. Izumoring, *J. Biosci. Bioeng.,* 2004, **97,** 89.
9 G. Gumina, G.-Y. Song, C.K. Chu, *Microbiol. Lett.,* 2001, **202,** 9.
10 B. Kamm, *Angew. Chemie Int. Ed.,* 2007, **46** 5056.
11 F. Ju, D. Vandervelde, E. Nikolla, *ACS Catal.,* 2014, **4**, 1358.
12 H.S. El Khadem, S. Ennifar, H.S. Isbell, *Carbohydr. Res.,* 1987, **169,** 13.
13 B.Y. Yang, R. Montgomery, *Carbohydr. Res.,* 1996, **280,** 27.
14 T. Tanase, F. Shimizu, M. Kuse, S. Yano, M. Hidai, S. Yoshikawa, *Inorg. Chem.,* 1988, **27,**4085.
15 S. Takizawa, H. Sugita, S. Yano, S. Yoshikawa, *J. Am. Chem. Soc.,* 1980, **102,** 7969.
16 S.J. Angyal, *Top. Curr. Chem.,* 2001, **215**, 1.
17 V. Bílik, L. Stankovic, *Chem. Zvesti.,* 1973, **27**, 544.
18 V. Bílik, *Chem. Zvesti.,* 1972, **26**, 372.
19 V. Bilik, I. Knezek, *Chem. Pap.,* 1990, **44**, 89.
20 V. Bilik, L. Petrus, V. Farkas, *Collect. Czechoslov. Chem. Commun.,* 1978, **43,** 1163.
21 B.K. Chethana, D. Lee, S.H. Mushrif, *J. Mol. Catal. A. Chem.,* 2015, 410, 66.
22 Y. Ren, M. Wang, X. Chen, B. Yue, H. He, *Materials (Basel),* 2015, **8,** 1545.
23 K.U. Nandhini, J.H. Mabel, B. Arabindoo, M. Palanichamy, V. Murugesan, *Micropor. Mesopor. Mater.,* 2006, **96**, 21.
24 G.S. Kumar, M. Vishnuvarthan, M. Palanichamy, V. Murugesan, *J. Mol. Catal. A Chem.,* 2006, **260**, 49.
25 Y.Y. Liu, K. Murata, M. Inaba, N. Mimura, *Catal. Commun.,* 2003, **4,** 281.
26 G. Karthikeyan, A. Pandurangan, *J. Mol. Catal. A Chem.,* 2009, **311,** 36.
27 J. Arichi, M.M. Pereira, P.M. Esteves, B. Louis, *Solid State Sci.,* 2010, **12,** 1866.
28 X. Han, W. Yan, K. Chen, C.-T. Hung, L.-L. Liu, P.-H. Wu, S. -J. Huang, S.-B, Liu, *Appl. Catal. A Gen.*, 2014, **485**, 149.
29 J. Chen, L. Hua, W. Zhu, R. Zhang, L. Guo, C. Chen, H. Gan, B. Song, Z. Hou, *Catal. Commun.,* 2014, **47,** 18.
30 S. Ivanova, ISRN Chem. Eng. 2014 Article ID 963792, 13 pages.
31 W. He, S. Li, H. Zang, G. Yang, S. Zhang, Z. Su, Y. Lan, *Coord. Chem. Rev.,* 2014, **279**, 141.
32 H.N. Miras, L. Vila-Nadal, L. Cronin, *Chem. Soc. Rev.,* 2014, **43,** 5679.
33 A. Mirzaei, M.; Eshtiagh-Hosseini, H.; Alipour, M.; Frontera, *Coord. Chem. Rev.,* 2014, **275** 1.
34 B. Santoni, M.-P.; Hanan, G.S.; Hasenknopf, *Coord. Chem. Rev.,* 2014, **281**, 64.
35 E. Du, D.; Yan, L.; Su, Z.; Li, S.; Lan, Y.; Wang, *Coord. Chem. Rev.,* 2013, **257**, 702.
36 U.B. Mioč, R.Ž. Dimitrijević, M. Davidovic, Z.P. Nedic, M.M. Mitrovic, P. Colomban, *J. Mater. Sci.,* 1994, **29,** 3705.
37 J.F. Keggin, *Proc. R. Soc. London Ser. A.,* 1934, **144**, 75.
38 J. Dupont, *J. Braz. Chem. Soc.,* 2004, **15**, 341.
39 S.J. Angyal, *Angew. Chemie - Int. Ed.,* 1969, **8**, 157.
40 A. Cybulski, B.F.M. Kuster, G.B. Marin, *J. Mol. Catal.,* 1991, **68**, 87.
41 A. Kiersztan, K. Winiarska, J. Drozak, M. Przedlacka, M. Wegrzynowicz, T. Fraczyk, J. Bryla, *Mol. Cell. Biochem.,* 2004, **261,** 9.
42 Y. Karlish, D.S.J. Shechter, *Nature.,* 1980, **284,** 556.
43 M.T. Pope, A. Müller, *Angew. Chem., Int. Ed.,* 1991, **30,** 34.
44 M. Watanabe, Y. Aizawa, T. Iida, C. Levy, T.M. Aida, H. Inomata, *Carbohydr. Res.,* 2005, **340,** 1931.
45 M.J. King-Morris, A.S. Serianni, *J. Am. Chem. Soc.,* 1987, **109,** 3501–3508.
46 V. Bilik, L. Petrus, *Chem. Zvesti.,* 1979, **33,** 114.
47 H. Wu, *J. Biol. Chem.,* 1920, **43,** 189.

48 G. Ranga Rao, T. Rajkumar, B. Varghese, *Solid State Sci.,* 2009, **11,** 36.
49 T. Rajkumar, G. Ranga Rao, *Mater. Lett.,* 2008, **62,** 4134.
50 T. Rajkumar, G.R. Rao, *J. Chem. Sci.,* 2008, **120,** 587.
51 M.C. Burla, R. Caliandro, M. Camalli, B. Carrozzini, G.L. Cascarano, L.G.C. De Caro, G. Polidori, R. Spagna, *J. Appl. Crystallogr.,* 2005, **38,** 381.
52 G.M. Sheldrick, *Acta Crystallogr. Sect. A.,* 2008, **64,** 112.

